Twelfth USA/Europe Air Traffic Management Research and Development Seminar (ATM2017)

Wind Efficient Path Planning and Reconfiguration of UAS in Future ATM

Leopoldo Rodriguez, Fotios Balampanis, Jose A. Cobano, Ivan Maza, Anibal Ollero
Robotics Vision and Control Group
University of Seville
Seville, Spain
Email: lrodriguez15, fbalampanis, jacobano, imaza, aollero@us.es

***Abstract*—Integration on Unmanned Aerial Systems (UAS) into future airspace is one of the greatest challenges in Air Traffic Management. The use of UAS for covering wide areas involves the consideration of airspace restrictions, obstacle avoidance and others which result in complex shapes that need to be partitioned smartly to ensure coverage. Another important element for consideration in the generation of safe and efficient trajectories of UAS is the wind field. Typically, in severe wind scenarios wind is considered often a hazardous condition. However, recent studies show that proper identification of the wind field may be used to increase the energy efficiency of the mission. This paper presents a novel method of area decomposition and partition that ensures coverage by generating a triangular mesh to optimize the coverage in the presence of urban areas, airspace restrictions or even the presence of an obstacle. The waypoint sequencing considers the wind field in order to adjust it online so that there is an energy gain with the identified wind speed. For this purpose, an innovative method for wind identification is proposed which analyses the statistical behavior of wind vector estimates in order to identify specific features and characterize given models. Given the design philosophy and architecture, this system can be integrated into next generation autonomous UAS flight management systems as part of the waypoint sequencing and trajectory optimization functions. A test case in the north-Seattle area is presented, which is simulated using a 6DOF model with different wind scenarios which resulted into considerable energy gain either by heeding the wind field during the waypoint sequencing and during the mission execution. Results show that there is a significant improvement on the energy efficiency with an energy consumption reduced by 10% in the presence of wind.**

I. Introduction

There are numerous ongoing research efforts which intend to provide the necessary requirements and procedures for the safe integration of UAS into non-segregated airspace in the context of the future Air Traffic Management (ATM) system, proposed in the Next Generation Air Traffic Management System (NextGen) and the Single Sky European Research (SESAR). Potential research and commercial UAS applications including goods delivery, search and rescue, and others, require a precise set of rules to ensure safety and reliability of the involved actors. In the context of applications which require area coverage in a non-segregated airspace, there are many aspects which need to be considered. Smart path planning is a key area that needs to be studied in order to ensure that any given task does not compromise the safety of the airspace in which is being performed. Current and future ATM imply complex and dynamic areas which represent numerous challenges in mission planning. Regarding light and small UAS, the National Aeronautics and Space Administration (NASA) has proposed the development of the Unmanned Air Traffic Management (UTM) [1] system for Low-Altitude UAS as a response to safely manage UAS in airspace that is and will be not regulating by the Federal Aviation Administration FAA. This effort involves a the participation of very important partners such as Amazon, Google, Lockheed Martin Corporation, Honeywell, etc. In addition of this set of rules one important concern of the airspace that is managed by the civil authority is how to provide a reliable Detect-and-Avoid capability as exposed by Haessig et al. [2], in which technologies such as Autonomous Dependent System-Broadcast (ADS-B) is explored as a means to resolve potential conflicts with cooperative obstacles. There are vast studies about such as the ones presented by Cordon et al. and Paczan et al. that provides an insight, on the systems perspective, of different aspects of the integration of UAS in both NextGen and SESAR contexts [3], [4]. In [3] the authors present the requirements of the interfaces that are needed for the different phases of flight of a UAS including the mission/flight preparation, as defined by the SESAR Concept of Operations (CONOPS) [5]. The Business or Mission Development Trajectory (BDT/MDT) is a key element on the future ATM operations, since mission planning, specially in areas in which the air traffic is dense, represents a considerable challenge.

One important element that can be considered in the early stages of mission planning, and has proven to affect the operation of all types of UAS, is the weather data [6], particularly the wind field. Nowadays, the use of Commercial-On-The-Shelf (COTS) components permits that the UAS navigation systems, even those classified as small or very light, provide to the users very accurate information on their state vector. However, the use of sensors to determine accurately the wind vector during the flight are expensive and does not provide a significant impact neither during the mission planning nor during the early stages of flight, in which accurate knowledge of the wind field may result into a more comprehensive path planning. Different research efforts, such as the one presented by Langelaan et al. in [7] and Wenz et. al. [8] present methods for wind estimation with low-cost sensors even considering

hazardous wind conditions. The instantaneous online estimation of the wind vector at any stage of flight, or during the pre-fight operations may not be sufficient to take advantage of the wind field to increase flight efficiency. The knowledge of hazardous wind conditions, which can be even inferred with weather reports or by observation, may impose restrictions in the use of UAS, even in segregated airspace. Nevertheless, the use of wind as a means to harvest energy in order to increase the efficiency has been a subject of research such as in [9]. By characterizing the wind field and identifying punctual phenomena such as wind-shear or thermals, the UAS may gain energy that permit to fulfill its mission with less fuel or to increase the duration of flight. In the cases presented in the literature [7], [9], and also in those that has been studied by the authors [10], the identification of wind is performed without any restriction in airspace. Therefore, it has been noticed that the integration of the wind identification with the path planning problem has to be taken into account for future ATM and UTM UAS operations.

The path planning problem and wide area coverage represents by itself a challenge if the complex shapes of airspace are taken into account. The plentiful restrictions, the consideration of static and moving obstacles, specially in operations close to urban areas, and the potential appearance of sudden air traffic restrictions require complex algorithms to quickly respond to the eventuality and prioritizing the mission accomplishment. As it is mentioned before, the wind field identification may result into the imposition of greater restrictions which will add complexity to the area decomposition, path planning (waypoint sequencing) or the path re-planning in an ongoing mission. However, if the wind field is identified it also may represent an advantage to increase the energy efficiency throughout the mission. Area decomposition and path planning problems have been widely studied before [11] and the use of algorithms such as boustrophedon movements typically represent solutions which do not ensure 100% coverage or complex areas. The authors have previously proposed an area decomposition method [12] [13] which seeks complete coverage waypoint plans and considers potential airspace restrictions regardless its shape, allowing the reconfiguration of the decomposed area and the waypoint re-sequencing considering different aspects or weights.

The purpose of this paper is to merge the area decomposition and path planning problem with a wind identification method in order to provide a mission planning and reconfiguration solution that considers the complex shapes of current and future airspace to ensure the highest possible coverage, also taking into account the efficiency and duration of the mission by acknowledging the identification of the wind field as a potential solution.

II. UAS-Based Wind Field Identification

The wind field identification problem, as proposed in [10], involves two stages. One that identifies the instantaneous wind field at a given rate and other that performs a statistical analysis to these estimates in order to identify wind features, which can be as simple as constant wind or as complex as discrete and continuous gusts or wind shear.

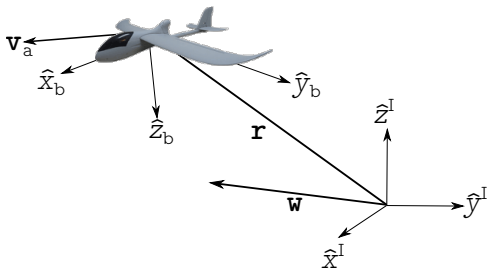

Fig. 1. UAS located in an inertial frame.

A. Wind Vector Estimation

The wind vector estimation is performed with a Direct Computation (DC) method. It consists in the use of the Global Navigation Satellite System (GNSS) navigation solution together with the air mass relative speed in order to determine the wind vector estimate without the use of a Bayesian filter.

Let a UAS to be located in a vector $\mathbf{r}$ in an inertial frame $\mathbf{I}$ with unit vectors defined as $(\hat{x}^I, \hat{y}^I, \hat{z}^I)$. Heeding a body frame located in the UAS center of mass with unit vectors $(\hat{x}_b, \hat{y}_b, \hat{z}_b)$, the wind vector $\mathbf{w}$ with components (w_x, w_y, w_z) and the air-mass-relative velocity (absolute airspeed) $\mathbf{v}_a$ are shown in Fig. 1.

From this point, one can infer the total velocity, based on the computation of the so-called speed triangle $\dot{\mathbf{r}}$ in the inertial frame as shown in (1):

$$\dot{\mathbf{r}} = \mathbf{v}_a + \mathbf{w} \tag{1}$$

Therefore, the wind vector $\mathbf{w}$ can be calculated in the inertial frame as in (2):

$$\begin{bmatrix} w_x \\ w_y \\ w_z \end{bmatrix}_{\mathbf{I}} = \begin{bmatrix} \dot{x} \\ \dot{y} \\ \dot{z} \end{bmatrix}_{\mathbf{I}} - (\mathbf{C}_{\mathbf{I}}^{\mathbf{b}})^{-1} \begin{bmatrix} u \\ v \\ w \end{bmatrix}_{\mathbf{b}} \tag{2}$$

The ground position with coordinates $(\dot{x}, \dot{y}, \dot{z})_I$ can be obtained with good precision in the navigation solution of the GNSS system, which typically has a Kalman filter function embedded to increase the precision. The airspeed components (u, v, w) which are typically given in the body frame can be determined with the knowledge of angle of attack and sideslip, or with the use of an multi-axis airspeed sensor as proposed by Wenz et al in [8]. COTS autopilots have the capability to compute the airspeed, AOA and sideslip which is sufficient to determine the wind components with relative good precision.

The main source of error in (2) cannot be inferred easily since the sources of error are independent. However, in [7], the computation of the wind speed acceleration, which can be also observed in [10], permits the determination of the airspeed measurements as the most important source of error. It has been determined that there is no need of a Bayesian filter to keep the wind vector estimation error bounded within

acceptable limits (between 0.7 m/s and 1 m/s for low flight path angles and without GNSS augmentation) [7].

B. Wind Field Prediction

In order to characterize the surrounding wind field, we can consider a wind field as the "sum" of four features: constant wind in a given direction, wind shear, discrete gusts and continuous gusts. The Wind Identification System (WIS) proposed by the authors in [10] performs a statistical analysis of accumulated wind estimates together with off-board information such as weather reports or a wind database.

Other important considerations that need to be taken into account are that wind measurements are typically distributed altitude-wise following a Weibull distribution. Given a data set of wind vector estimations $\mathbf{W} = (W_1, ..., W_n)$, the Weibull distribution can be expressed as:

$$f(\mathbf{W}) = \frac{\kappa}{\nu}\left(\frac{W}{\nu}\right)^{(\kappa-1)} e^{\frac{W}{\nu}\kappa} \tag{3}$$

where κ and ν are respectively the shaping and scaling parameters of the Weibull distribution.

From here, one can infer the most probable wind speed $\|\mathbf{w}\|_r$ at a particular location as a function of κ and ν:

$$\|\mathbf{w}\|_r = \nu\left(1 - \frac{1}{\kappa}\right)^{\frac{1}{\kappa}} \tag{4}$$

The identification of the Weibull parameters to calculate the wind speed magnitude is not trivial, therefore, a solution which has been implemented as in [10] is to use a Genetic Algorithm (GA) in order to estimate the Weibull parameters and to determine the most probable wind speed at a given location. An implementation of the GA to find the Weibull parameters can be found in [10].

Once the Weibull parameters are identified in altitude groups, a statistical analysis of the running mean and standard deviation of the wind estimates is performed in order to fit the wind estimates into feature models either by analyzing the wind magnitude change over altitude with an Empirical Power Law (EPL) or by performing a short term Gaussian regression to characterize complex features. The selected models are based on the U.S. Military Specification MIL-F-8785C [14], [15].

1) Wind Shear Identification: In the presence of a Wind Shear, wind estimates show a growth in the airspeed over altitude as shown in Fig 2. It is represented by the following expression:

$$\|\mathbf{w}\|_{\text{shear}} = \mathrm{W}_{20}\frac{\ln\frac{h}{z_0}}{\ln\frac{6.096}{z_0}}, 1\text{m} \leq h \leq 300\text{m} \tag{5}$$

Shear is a typically undesired phenomena in terminal area operations for manned aircraft. However, in the case of UAS and while operating in the UTM, it can be useful if the surface layer is identified properly, i.e. the altitude in which the wind speed is decreasing faster allowing a energy gain in the form of speed or altitude.

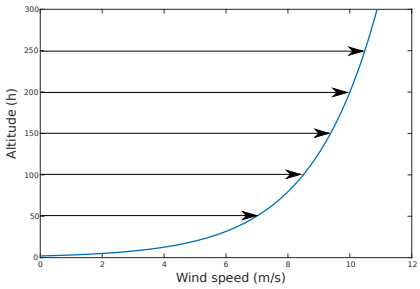

Fig. 2. Wind shear model.

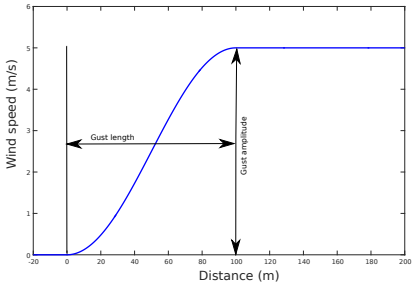

Fig. 3. Discrete gust model.

If a group of most probable wind speeds $\Omega = W_m p_1, W_m p_2, ..., W_m p_n$ can be fitted with a polynomial approximation into the empirical power law, then the WIS assumes that there is a presence of shear on the system. By analyzing the components of the wind vector estimates, the wind direction can be inferred by averaging the direction cosines between them.

2) Discrete Gust Identification: The discrete gust can be seen as an increase of the wind velocity magnitude within a distance. The considered model is the $1-\cos$ as in [14], [15]:

$$\|\mathbf{w}\|_{\text{gust}} = \begin{cases} 0 & x < 0 \\ \frac{Wm}{2}\left(1 - \cos\frac{\pi x}{d_m}\right) & 0 \leq x \leq d_m \\ W_m & x > d_m \end{cases} \tag{6}$$

And it is represented in Fig. (3)

In order to characterize the discrete gust one can refer to the work presented by Zbrozek [17] in which the distribution of discrete gusts, while knowing the power spectrum of normal acceleration, can be utilized in order to determine the intensity of the discrete gust by a continuous distribution of Root Mean Squared (RMS) turbulence. Hence, the analytic expression for probability density distribution of a gust velocity is:

$$\hat{f}(\sigma_w) = \sqrt{\frac{2}{\pi}\frac{1}{b}\exp\left(-\frac{1}{2}\left(\frac{\sigma_w}{b}\right)^2\right)} \tag{7}$$

Therefore, by observing the RMS distribution of the wind estimates one can determine the intensity if the gust is considered a stationary process.

3) Continuous Gust Identification: For the continuous gust, the Dryden spectral representation is used. This representation, also approved in [14], [15] treats the linear and angular wind velocities as spatially varying stochastic processes in which each component is defined by a power spectral density. Therefore, the power spectral densities Φ for linear velocities (u_g, v_g, w_g) and angular velocities are shown in (8) and in (9).

$$\begin{bmatrix} \Phi_{u_g}(\Omega) = \sigma_u^2 \frac{2L_u}{\pi} \frac{1}{(1+L_u\Omega)^2} \\ \Phi_{v_g}(\Omega) = \sigma_v^2 \frac{2L_v}{\pi} \frac{1+12(L_v\Omega)^2}{(1+4(L_u\Omega)^2)^2} \\ \Phi_{w_g}(\Omega) = \sigma_w^2 \frac{2L_w}{\pi} \frac{1+12(L_w\Omega)^2}{(1+4(L_w\Omega)^2)^2} \end{bmatrix} \tag{8}$$

$$\begin{bmatrix} \Phi_{p_g}(\omega) = \frac{\sigma_w^2}{2VL_w} 0.8 \left(\frac{2\pi L_\omega}{4b}\right)^{\frac{1}{3}} \\ \Phi_{q_g}(\omega) = \frac{\pm\left(\frac{\omega}{V}\right)^2}{1+\left(\frac{4b\omega}{\pi V}\right)^2} \Phi_{w_g}(\omega) \\ \Phi_{q_g}(\omega) = \frac{\mp\left(\frac{\omega}{V}\right)^2}{1+\left(\frac{3b\omega}{\pi V}\right)^2} \Phi_{v_g}(\omega) \end{bmatrix} \tag{9}$$

where σ_i is the root-mean-square vertical or lateral gust velocity and L_i is an integral length scale of the turbulence eddies in the ith. velocity or angular component. Ω is the spatial frequency and b represents the aircraft wingspan.

Trying to characterize the spectral density definitions in order to predict a turbulence is a complex problem that requires high computational power and the results may not be useful for online use. However, a standard Gaussian Process (GP) regression can be incorporated in order to perform a short-term prediction to determine a covariance vector $\mathbf{q}(\mathbf{X}, x)$ and a linear prediction $\bar{p}(X)$ of a linear combination of the wind estimates in the ith direction. The expression of the prediction is:

$$\bar{p}(X) = \mathbf{q}(x, \mathbf{X}) \left[\mathbf{Q}(\mathbf{X}, \mathbf{X}) + \sigma_n^2 \mathbf{I}\right]^{-1} \hat{\mathbf{W}}_z \tag{10}$$

where $\mathbf{q}(x, \mathbf{X})$ is the covariance vector between two observations at location $\mathbf{X}$, $\mathbf{Q}(\mathbf{X},\mathbf{X})$ is the covariance matrix and σ_n^2 is the measurement noise covariance. Additional details on the implementation of the regression can be found in [10].

III. Complex Area Partitioning Considering Aerial Restrictions.

The increased interest of UAS usage for commercial purposes reflects on several mission scenarios which surpass the use of specific waypoint airways. These missions are often handled by the means of a grid decomposition of areas in order to accomplish complete coverage [11], for instance in crop spraying or aerial photography. As we've shown in a previous study [12], complex scenarios and geographic attributes are not treated properly by the use of a simple grid decomposition of an area. More specifically, coastal area tasks with their numerous no fly zones or complex shores, impose a dynamical approach which has been developed in the context of the MarineUAS project.

In a test case scenario area as seen in Fig.4, several heterogeneous UAS have the task of covering the area in order to obtain sea life information by using their sensors.

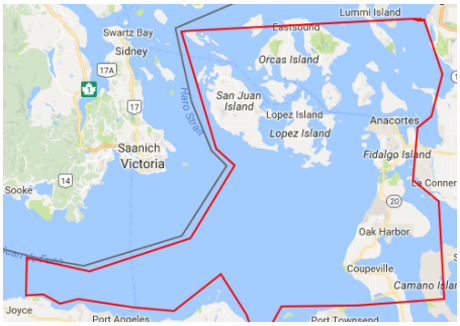

Fig. 4. A test case area, north of Seattle. The red polygon defines the mission area whereas several other restrictions apply, as can be seen in the next figures.

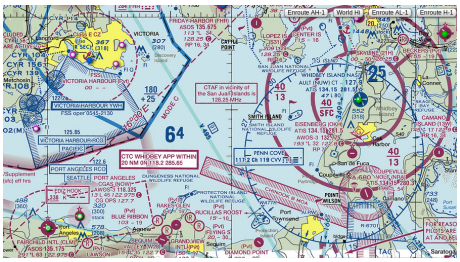

Fig. 5. Several low altitude restrictions apply in the area, like those that can be seen on the bottom right part. Moreover, the system must be capable to respond in any online restriction. Screenshot is a courtesy of SkyVector.com

In order to perform a fair and successful partitioning of the configuration spaces for each UAS, respecting their relative sensing capabilities, like their Field of View (FoV), as also as the strict borders of the area or future airspace restrictions, an initial Constrained Delaunay Triangulation (CDT) is proposed.

A CDT introduces forced edge constrains as part of the input and in such a way, complex areas can be triangulated, creating a triangular mesh. Then, each centroid of every triangle can be considered as a waypoint in the flight plan. Moreover, every triangle can be given a cost, based on several task,area or agent related criteria. As we will describe, this cost can be used for wind information and will further facilitate the extraction of waypoint flight plans.

Consider the region presented in Fig.4 as $\mathcal{C}$, including obstacles, as shown in Fig.5. For waypoint list planning, this area is treated as a two dimensional grid such that $\mathcal{C} = \mathbf{R}^2$, where $\mathcal{C}_{obs}$ are the restricted areas and $\mathcal{C}_{free} = \mathcal{C} \setminus \mathcal{C}_{obs}$ is the area to be partitioned for the UASs. By triangulating and partitioning $\mathcal{C}_{free}$ for M vehicles in a sum of triangles (ψ) such that

$$\mathcal{C}_{free} = \sum_{i=1}^{M} \sum_{j=1}^{N} \psi_{ij} \ , \tag{11}$$

the waypoint planning is actually a graph search problem of N nodes organized in the CDT. The algorithmic strategies presented in [13] are not computationally expensive and permit the online reconfiguration and planning for either detect and avoidance purposes, task updates or emergency situations.

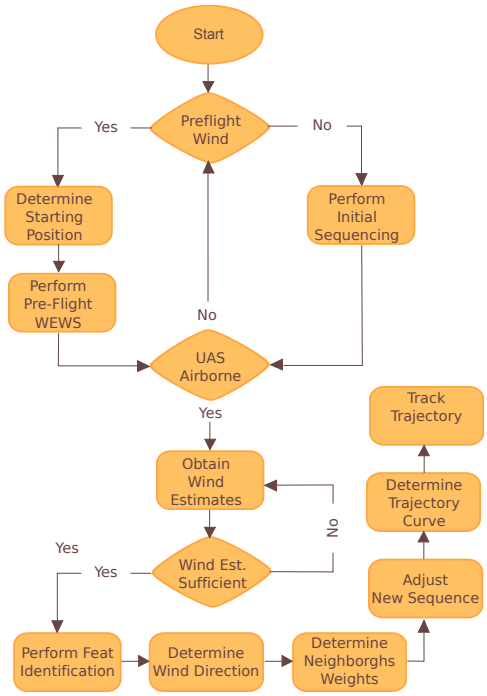

Fig. 6. High level view of the WEWS algorithm.

IV. Wind Efficient Waypoint Sequencing

In order to perform the wind predictions, as described in Section II-B, wind estimations have to be stored until a sufficient number of them allows such process. This process takes in average 60 s from the moment the UAS goes airborne [10].

During pre-flight phase, the meteorological reports and the use of external sensors, such as an anemometer, allow an estimation of the predominant wind direction and to do a initial wind-based sequencing in order to improve the flight efficiency.

The Wind Efficient Waypoint Sequencing (WEWS) process weights the cells of the decomposed area in such a way that prioritizes the information on the wind field in two stages: the first one aims to determine the predominant wind direction in the presence of constant wind, shear and/or discrete gusts and determines a sequence in which the sequence tries to keep a positive component aligned to the wind velocity. The other proposed process intents to provide information to the autopilot in order to adjust the trajectory on a waypoint-to-waypoint basis to maximize the use of the wind as a means of gaining energy. The WEWS high level process is depicted in Fig. 6.

The initial sequencing is considered as an iteration into the Shared Business or Mission Trajectory (SBT/SMT) process. However, during the execution of the mission, the trajectory may suffer adjustments which are to be used in the update of the Reference Business or Mission Trajectory (RBT/RMT). During anytime during the mission execution, the path might suffer from temporary restrictions or even the appearance of an

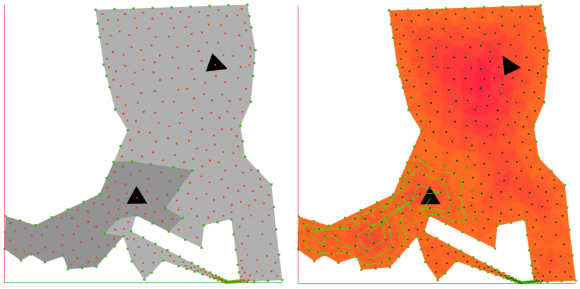

Fig. 7. North Seattle area with a flight restriction on the bottom right. Left: initial partition for 2 UASs, having an 80% and 20% relative area coverage capabilities. Black triangles represent the initial positions of the UASs, while the red dots represent the waypoints. The two configuration spaces are distinguished by the different shades of grey. Right: Borders to center cost applied to each cell and a coverage flight plan has been extracted for one of the UASs.

obstacle. The area decomposition and partitioning algorithms are able to reconfigure the waypoint sequence accordingly ensuring coverage of the area still with the wind information as part of the weight.

The energy as a function of the trajectory $\mathbf{q}(t)$:

$$\bar{E}(\mathbf{q}(t)) = \int_0^T \left[c_1 \|\mathbf{v}(t)\|^3 + \frac{c_2}{\|\mathbf{v}(t)\|}(1 + \frac{\|\mathbf{a}(t)\|^2 - \mathbf{m}}{g^2}) \right] dt + \frac{1}{2} m(\|\mathbf{v}(T)\|^2 - \|\mathbf{v}(0)\|^2) \tag{12}$$

where

$$\mathbf{m} = \frac{(\mathbf{a}^T(t)\mathbf{v}(t))^2}{\|\mathbf{v}(T)\|^2} \tag{13}$$

$\mathbf{v}(t)$ corresponds to the first derivative of the trajectory function:

$$\mathbf{v}(t) \triangleq \dot{(q)}(t) \tag{14}$$

$\mathbf{a}(t)$ is the second derivative of the trajectory function:

$$\mathbf{a}(t) \triangleq \dot{(q)}(t) \tag{15}$$

and g is the gravitational constant.

In general, avionics power consumption is significantly smaller in proportion to the propulsion energy. Therefore only kinematic related components are included into (12).

V. Test Cases, Simulations and Results

The area of Fig.4 has been chosen as a test case, by taking into consideration a simple aerial restriction as can be seen in Fig.5. The area has been partitioned for two UASs, having the same FoV but different coverage capabilities. A coverage waypoint flight plan has been extracted for one of them, having as a sequence criterion the outer to inner complete coverage (Fig.7). The simulated experiments show that the resulting trajectories manage to respect the aforementioned restrictions while successfully performing the coverage task (Fig.8).

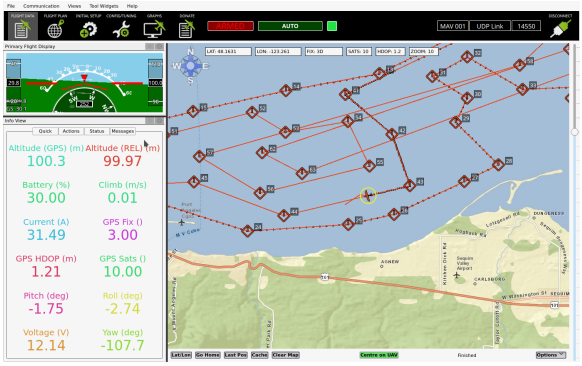

Fig. 8. An APM screenshot during flight.

For simulation purposes the UAS with 20% relative area coverage capability was selected. The simulated platform corresponds to the Aerosonde UAV (see Fig. 9. Its characteristics are enumerated in Table I.

A 6DOF model was selected in order to perform Software-In-The-Loop (SITL) experiments with the WEWS algorithms in place. Simulations were performed using the MATLAB/SIMULINK®. environment together with the Pixhawk SITL environment.

Three scenarios are considered, the first one decomposes the area as in [12], sequencing the waypoints from the edges to the center in order to ensure full coverage. The second scenario considers the presence of sustained wind. Finally the third scenario considers shear and gust phenomena.

TABLE I
AEROSONDE UAV CHARACTERISTICS

Length	1.7 m
Width	2.9 m
Height	1.97 m
Weight (MTOW)	25 kg
Maximum Speed	140 knot
Maximum Range	3000 km
Maximum Ceiling	4500 m (14760 ft)

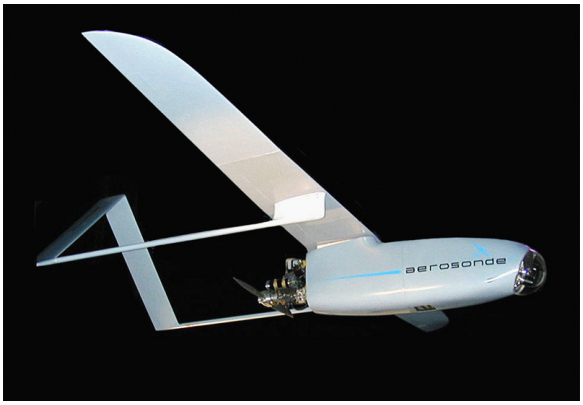

Fig. 9. Aerosonde UAV.

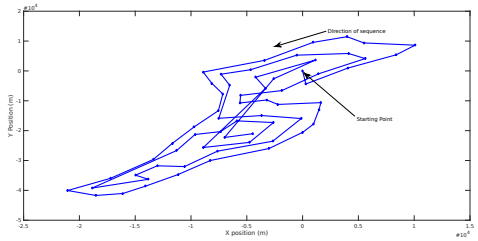

Fig. 10. Initial area decomposition showing the starting point and the wind direction.

TABLE II
FIRST SEQUENCING SIMULATION RESULTS

Flight Duration	3.2 h
Medium Altitude	100 m ASL
Total Energy Consumption	≈22385.66 W/h
Average Wind Speed	0 m/s
Average Airspeed	20.93 m/s

A. *First scenario: zero wind consideration*

Taking the UAS located at the bottom left of Fig. 7. The proposed area is decomposed and sequenced initially as indicated in Fig. 10, in which the coordinates are expressed as relative position to the starting point. Note that this base sequencing does not consider prior information of the wind field.

While executing this trajectory the approximated resulted energy as per 12 in a Software-In-The-Loop (SITL). The results of the simulation are shown in Table II

For the energy calculation a standard gasoline engine with a displacement of 55 CC and a power of 5.6 HP was considered as a test case. Hence, the avionics consumption is not included in the calculation.

B. *Second scenario: constant wind consideration*

For the second scenario, an average sustained wind of 5 m/s is considered with a wind direction of (-90^{o}). This allows to appreciate the impact of the wind in the initial waypoint sequencing. If this wind is considered then the system tries to minimize the amount of times that the trajectory of the aircraft has a negative component relative to the direction of the wind. In addition, the sustained wind was identified and characterized as per the Weibull distribution indicated in (3).

The resulting sequencing with the online adjustment is depicted in Fig. 11. In addition, the identified wind velocity with the corresponding Weibull characterization can be observed in Fig. 12.

The simulation results and energy consumption are shown in Table III. It can be observed and improvement of approximately 11% in the energy consumption. Note that during the simulation the flight mode was on speed control, therefore, the UAS travels a similar distance with a different sequence. Hence, the flight duration is not significantly impacted. Note that the average airspeed is decreased due to the wind effect.

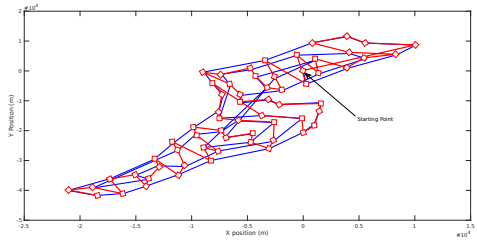

Fig. 11. Area decomposition considering sustained east wind.

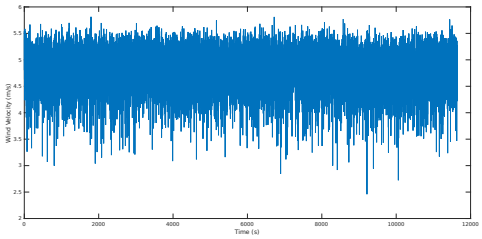

Fig. 12. Estimated wind speed over time with a mean value of 5 m/s.

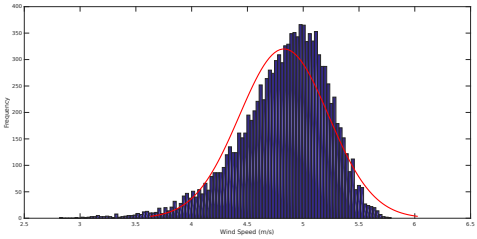

Fig. 13. Distribution of wind estimates following a Weibull shape.

TABLE III
SECOND SEQUENCING SIMULATION RESULTS

Flight Duration	3.16 h
Medium Altitude	100 m ASL
Total Energy Consumption	≈19913.408 W/h
Average Wind Speed	5 m/s
Average Airspeed	16.74 m/s

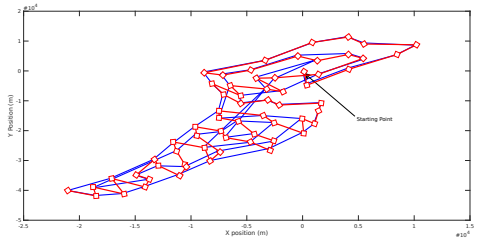

Fig. 14. Area decomposition considering discrete gust.

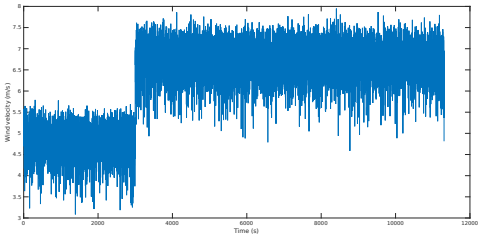

Fig. 15. Estimated wind speed over time with a mean value of 5 m/s.

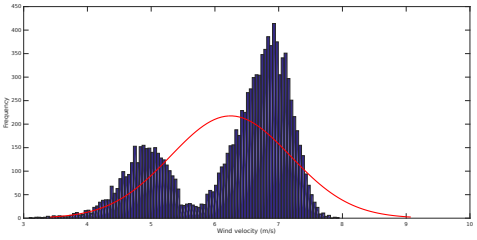

Fig. 16. Distribution of wind estimates following a Weibull distribution.

TABLE IV
SECOND SEQUENCING SIMULATION RESULTS

Flight Duration	3.19 h
Medium Altitude	100 m ASL
Total Energy Consumption	≈20421.783 W/h
Average Wind Speed	6.24 m/s
Average Airspeed	15.23 m/s

During the simulation, online adjustments are done in the trajectory allowing reshaping the remaining waypoint sequencing. The main inconvenience of this is that there are sharp turns that may result into higher energy consumption considering the full dynamics and the actual trajectory tracking.

C. Second scenario: gust wind consideration

The last scenario considers the presence of gust and shear. however, since there are no changes in altitude the shear does not affect directly the energy gain. The simulation starts with no knowledge of the wind field and after a minute of flight, the first wind predictions start to occur. Once the system determines the wind velocity and direction (5 m/s, -90^o) the algorithm starts to reconfigure the path during the first part of the flight. At 3000 s, a discrete gust of 2 m/s occurs which results into the increase of the wind velocity magnitude. The direction of the wind is also affected hence the system performs a more severe reconfiguration of the flight path. The identification of the gust can be determined by detecting the increase of the wind speed (see Fig. 15) and also with the generation of two Weibull distributions as seen in Fig. 16.

The simulation results can be observed in Table IV. In here a energy improvement of 8% was observed. Note that the waypoint sequence starts as in Fig. 10, however as the wind is identified and the gust is detected there are significant changes on the sequence.

In the two cases, the energy improvement occurred only by rearranging the original waypoint sequence. Even though some overlapping of way points may be observed, there is still a significant improvement by considering the wind force.

VI. Conclusion and Future Work

The presented algorithms for area decomposition, waypoint sequencing and wind identification are a promising combination for generating wind efficient trajectories for UAS in future airspace. Normally, a decomposition method takes little consideration of the wind phenomena as an aid to improve the energy efficiency. The cell weighting method allows the generation online reconfiguration of the intended waypoint sequence considering potential airspace restrictions in the context of current and next generation airspace. The designed architecture allows an easy incorporation into next generation Business or Mission Trajectory (B/MT) procedures. The area decomposition ensures the maximum coverage of a given area due to the triangular cells that permit the inclusion of complex shapes, which are given by the surface of the surveyed area and/or airspace restrictions. The results shows improvements up to 11% of efficiency with low winds and up to 9% in the presence of gust and shear with online sequence reconfiguration. Efficiency is one of the key aspects in future airspace with more stringent carbon-dioxide emission regulations, and the wind energy harvesting is a promising area for UAS operating in low altitudes in both the UTM and ATM systems. The incorporation of wind identification and smart area decomposition into UAS flight management functions shall permit a more efficient use of airspace even in hard meteorological conditions. Future work includes the incorporation of the described system to a trajectory generation system in order to determine, on a waypoint-to-waypoint basis, the 4D optimal trajectories for maximum energy gain given a wind field. This will allow a more realistic quantification of the energy harvested to the wind by generating soaring trajectory solutions even for the sharp turns that the sequencing system generates. The safety and reliability of UAS systems including COTS components allow identification of the wind vector and wind field with the necessary precision to perform the initial sequencing, online reconfiguration and trajectory optimization. In addition, a full test campaign is being prepared in order to validate and verify the different functions for safe-long duration missions.

Acknowledgment

This work has been supported by the MarineUAS project, funded by the European Commission under the H2020 Programme as part of the Marie Sklodowska Curie Actions (MSCA-ITN-2014-642153) and the AEROMAIN Project (DPI2014-5983-C2-1-R), funded by the Science and Innovation Ministry of the Spanish Government.

References

[1] UTM: Air Traffic Management for Low-Altitude Drones, National Aeronautics and Space Administration. Washington DC, United States of America, 2015.

[2] D.A. Haessig, R.T. Organ, M. Olive. " "Sense and Avoid" - What's required for aircraft safety", SoutheastCon 2016 . , Northfolk, VA. United States of America, March 30-April 3. 2016.

[3] R.R. Cordón, F. J. Saz, C. Cuerno. "RPAS Integration in Non-segregated Airspace: the SESAR Approach. Systems Needed for Integration", Fourth SESAR Innovation Days . Madrid, Spain, 25th 27th November 2014.

[4] N.M. Paczan, J. Cooper, E. Zakrewski. "Integrating Unmanned Aircraft Into NextGen AUtomation Systems", 31st Digital Avionics Systems Conference. Williamsburg, VA, United States of America, October 14-18, 2012.

[5] SESAR Concept of Operations Step 1, EUROCONTROL, SESAR Joint Undertaking. Brussels, Belgium, 2013.

[6] L. Nelson. "More than Just a Weather Forecast. The Critical Role of Accurate Weather Data in UAV Missions", Defense Update. United States of America, 2009.

[7] J.W. Langelaan, N. Alley, J. Neidhoefer. "WInd Field Estimaton for Small Unmanned Aerial Vehicles", AIAA Guidance, Navigation and Control Conference. Toronto, Canada, 2010.

[8] A. Wenz, T.A. Johansen, A. Cristofaro. "Combining model-free and model-based Angle of Attack estimation for small fixed-wing UAVs using a standard sensor suite" International Conference on Unmanned Aircraft Systems (ICUAS), 2016.

[9] A. Chakrabarty. J.W. Langelaan. "Flight Path Planning for UAV Atmospheric Energy Harvesting Using Heuristic Search", AIAA Guidance, Navigation and Control Conference. Toronto, Canada, 2010.

[10] L. Rodriguez. J.A. Cobano. A. Ollero "Small UAS-Based Wind Feature Identification System Part 1: Integration and Validation", Sensors 2017, 17(1).

[11] Galceran, E. and Carreras, M., 2013. A survey on coverage path planning for robotics. Robotics and Autonomous Systems, 61(12), pp.1258-1276.

[12] F. Balampanis, I. Maza, A. Ollero. "Area decomposition, partition and covarage with multiple remotely piloted aircraft systems operating in coastal regions" 2016 International Conference on Unmanned Aircraft Systems (ICUAS). Arlington, VA, United States of America, 2016, pp. 275-283.

[13] F. Balampanis, I. Maza, A. Ollero. "Coastal Areas Division and Coverage with Multiple UAVs for Remote Sensing" MDPI Sensors. Submitted for review. 2017.

[14] U.S. Department of Defense "Military Specification, Flying Qualities of Piloted Airplanes MIL-F-8785C", Department of Defense. Washington DC, United States of America, 1980

[15] U.S. Department of Defense "Handbook, Flying Qualities of Piloted Airplanes MIL-F-8785C", Department of Defense. Washington DC, United States of America, 1980

[16] C. Gao. "Autonomous Soaring and Surveillance in Wind Fields with and Unmanned Aerial Vehicle", PhD Thesis, University of Toronto. Toronto, Canada, 2015.

[17] J.K. Zbrozek. "The Relationship between the Discrete Gust and Power Spectra Representations of Atmospheric Turbulence With a Suggested Model of Low-Altitude Turbulence", Aeronautical Research Council Reports and Memoranda No. 3216 (1). Cranfield, United Kingdom, March, 1960.